

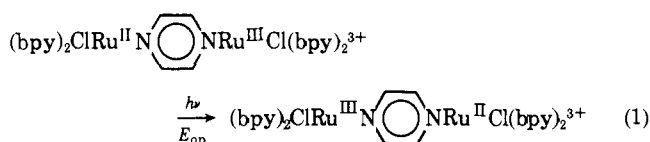
Medium and Distance Effects in Optical and Thermal Electron Transfer¹

Michael J. Powers and Thomas J. Meyer*

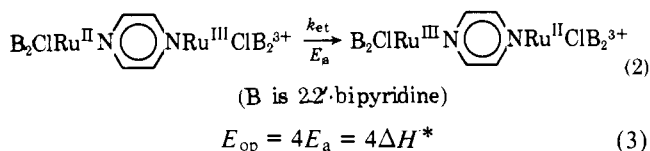
Contribution from the Department of Chemistry, The University of North Carolina, Chapel Hill, North Carolina 27514. Received March 9, 1979

Abstract: The series of dimers $(\text{bpy})_2\text{ClRu}(\text{L})\text{RuCl}(\text{bpy})_2^{2+}$ (bpy is 2,2'-bipyridine; L is pyrimidine, pyrazine, 4,4'-bipyridine, *trans*-1,2-bis(4-pyridyl)ethylene, and 1,2-bis(4-pyridyl)ethane) has been prepared. One-electron oxidation gives solutions containing the mixed-valence Ru(II)–Ru(III) dimers. For the mixed-valence dimers where the bridging ligand is unsaturated, intervalence transfer (IT) bands are observed in a series of polar solvents. The effect of the polarization properties of the solvent on the energies of the optical transitions, and by inference on the activation energies for related thermal processes, can be treated using a simple dielectric continuum model. The effect of the distance between redox sites can also be accounted for by making a relatively simple empirical correction to the continuum result. When extended to related outer-sphere electron-transfer reactions, the results for the mixed-valence ions show that in polar solvents close contact between reactants is energetically favored even for like charged ions and that there is no energetic basis for expecting that long-range electron transfer will occur.

In mixed-valence dimers where electronic coupling between redox sites is weak, the excess electron is usually found to be vibrationally trapped at one site at least in the equilibrium sense.² Low-energy absorption bands are frequently observed for such dimers which on the basis of their band shape and medium dependences can be assigned to metal–metal charge transfer (MMCT) or intervalence transfer (IT) absorption bands (eq 1).^{2c,3} Hush^{2a} and more recently Hopfield⁴ have

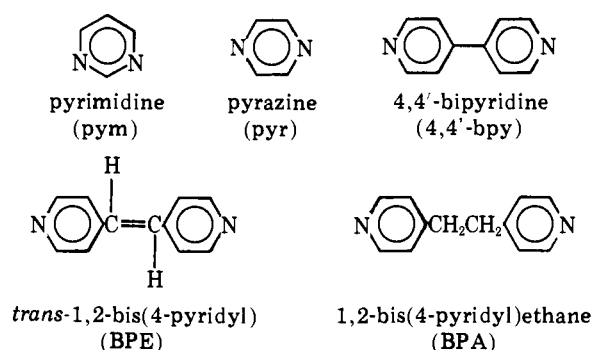


given theoretical treatments for optical electron-transfer processes. Assuming weak electronic coupling, harmonic oscillator vibrations, and a high temperature limit, the energy of the optical transition (E_{op}) in a symmetrical ion like $(\text{bpy})_2\text{ClRu}(\text{pyr})\text{RuCl}(\text{bpy})_2^{3+}$ (pyr is pyrazine) is given by eq 3. In eq 3 E_a is the energy of activation for the related thermal reaction (eq 2).



Because of the simple nature of eq 3, and the ease of measuring optical absorption bands, the appearance of MMCT or IT bands can be of great value in probing the microscopic details involved in both optical and thermal electron transfer. Earlier work with symmetrical mixed-valence ions^{2c} has explored the role of medium effects in inner-^{3a,5,6} and outer-sphere⁷ intramolecular electron transfer, has studied the effect of distance between redox sites,^{2c,6,8} and has led to the estimation of absolute electron transfer rate constants from the properties of IT bands.⁹

We report here the preparation of a series of ligand-bridged Ru(II)–Ru(II) dimers $\text{B}_2\text{ClRu}^{\text{II}}(\text{L})\text{Ru}^{\text{II}}\text{ClB}_2^{3+}$ (L = pyrimidine (pym), pyrazine (pyr), 4,4'-bipyridine (4,4'-bpy), *trans*-1,2-bis(4-pyridyl)ethylene (BPE), and 1,2-bis(4-pyridyl)ethane (BPA)). Oxidation of the dimers in solution gives mixed-valence Ru(II)–Ru(III) dimers. IT bands appear for the mixed-valence dimers in a series of polar solvents and the energies of the bands are used to test and modify a dielectric continuum model which accounts for the effects both of solvent polarization and distance between redox sites. Part of this work has appeared in a preliminary communication.⁸



Experimental Section

Measurements. Ultraviolet–visible and near-infrared spectra were recorded using Cary Models 14 and 17 and Bausch and Lomb Spectronic 210 spectrophotometers. Electrochemical measurements were routinely made at a platinum bead electrode, or vs. the saturated sodium chloride calomel electrode (SSCE) at 25 ± 2 °C, and are uncorrected for junction potentials. The measurements were made using a PAR Model 173 potentiostat for potential control and a PAR Model 175 universal programmer as a sweep generator for voltammetric experiments. The electrochemical measurements were performed in three-chamber electrochemical cells whose dimensions and construction have been described previously by Brown.¹⁰ The techniques employed for cyclic voltammetry, voltammetry, potentiometry, and coulometry as well as the criteria used to judge the electrochemical reversibility of the redox couples involved have also been described by Brown.¹⁰

Materials. Tetra-*n*-butylammonium hexafluorophosphate (TBAH) was generally used as supporting electrolyte for electrochemical experiments. It was prepared by standard techniques,¹¹ recrystallized three times from hot ethanol–water mixtures, and vacuum dried at 70 °C for 10 h.

Solvents used for near-infrared spectral measurements were purified according to published purification techniques.^{12,13} All other solvents used were reagent grade and used without further purification.

Deuterated solvents, used for near-infrared experiments, were purchased commercially (Stohler Isotope Chemicals, Inc.) and used without further purification.

Reagents. All chemicals used in the preparation of complexes were purchased commercially as reagent grade and used without further purification. Argon was scrubbed of oxygen by passing it through Drierite, a heated column containing catalyst R3-11 (Chemalog), followed by Drierite. Elemental analyses were performed by Galbraith Laboratories, Inc., Knoxville, Tenn., and by Integral Microanalytical Labs, Inc., Raleigh, N.C.

Preparation of Complexes. The preparations of the complex $(\text{bpy})_2\text{RuCl}_2 \cdot 2\text{H}_2\text{O}^{14}$ and the salts $[(\text{bpy})_2\text{ClRu}(\text{NO})](\text{PF}_6)_2^{15}$ and $[(\text{bpy})_2\text{XRu}(\text{L})](\text{PF}_6)_n \cdot m\text{H}_2\text{O}^{11,16}$ in which (L) = pym, pyr, 4,4'-bpy,

Table I. Elemental Analyses for the Salts [(bpy)₂ClRu(L)RuCl(bpy)₂](PF₆)_n·mH₂O

salt ^a	calcd				found			
	% C	% H	% N	% Cl	% C	% H	% N	% Cl
	Ru(II)-Ru(II)							
[B ₂ ClRu(pym)RuClB ₂](PF ₆) ₂ ·H ₂ O	41.10	2.98	10.89	5.51	41.13 ^b	2.51 ^b	10.60 ^b	
					40.16	2.72	10.65	5.47
[B ₂ ClRu(pyr)RuClB ₂](PF ₆) ₂	41.68	2.86	11.05		41.38 ^c	2.80 ^c	11.02 ^c	
[B ₂ ClRu(4,4'-bpy)RuClB ₂](PF ₆) ₂	44.69	3.00	10.42		44.47	3.08	10.26	
[B ₂ ClRu(BPE)RuClB ₂](PF ₆) ₂ ·2H ₂ O	44.42	3.30	9.96	5.18	44.24	3.11	9.96	
[B ₂ ClRu(BPA)RuClB ₂](PF ₆) ₂ ·2H ₂ O	44.39	3.44	9.96	5.04	43.41	2.86	9.97	4.30
	Ru(III)-Ru(III)							
[B ₂ ClRu(4,4'-bpy)RuClB ₂](PF ₆) ₄ ·2H ₂ O	35.96	2.66	8.39	4.25	35.71	2.72	8.82	5.09
[B ₂ ClRu(BPE)RuClB ₂](PF ₆) ₄ ·2H ₂ O	36.83	2.73	8.26	4.18	35.14	2.49	8.35	4.27

^a B is 2,2'-bipyridine. The ligands were shown above. ^b Taken from ref 17. ^c Taken from ref 3a.

BPE, and BPA and X = Cl⁻, NO₂⁻ (*n* = 1) or CH₃CN, py (*n* = 2), have been described previously.

The monomeric starting materials, [(bpy)₂ClRu(L)](PF₆), in which (L) = pym, pyr, 4,4'-bpy, BPE, and BPA, were purified by column chromatography, using either unactivated alumina (Fisher Scientific Co.) or cellulose (Baker Chemical Co., acid washed). Jacketed chromatography columns were used. A slurry of alumina in CH₂Cl₂ was poured into the column, and the complex, dissolved in CH₂Cl₂, was added dropwise to the top after settling. Mixtures of MeOH in CH₂Cl₂ were used as eluent. Initially 2% CH₃OH/CH₂Cl₂ was used followed by higher concentrations of CH₃OH to elute the first bands from the column which contained the desired products. There were impurities retained on the column. The most probable origins for the impurities were [(bpy)₂ClRuN₃], [(bpy)₂ClRu(S)](PF₆) (S = solvent), and [(bpy)₂ClRu(NO)](PF₆)₂. All of the impurities could be removed from the columns by washing with pure CH₃OH. Mixtures of CH₃CN (reagent grade) in benzene and in CH₂Cl₂ were also used successfully as eluents. The concentration of CH₃CN was generally 20–30%. In general, elution using CH₃CN was less desirable because of the problem of photochemical solvolysis reactions.

[(bpy)₂ClRu(L)RuCl(bpy)₂](PF₆)₂·*n*H₂O, (L) = pym,¹⁷ pyr,^{3a} 4,4'-bpy, BPE, and BPA.¹⁸ Preparations for the dinuclear complexes have appeared previously.^{3a,17,18} The preparations reported here represent modifications of the previous procedures. Specific examples are cited, but the same procedures were used for all the dimers.

[(bpy)₂ClRu(4,4'-bpy)RuCl(bpy)₂](PF₆)₂. **Route A.** [(bpy)₂-Ru(NO)Cl](PF₆)₂ (0.593 g, 0.771 mmol) was dissolved in 30 mL of acetone. KN₃ (0.063 g, 0.777 mmol) dissolved in a minimum amount of CH₃OH (~5 mL) was added dropwise to the solution. The solution was protected from light. After 15 min of stirring, 4,4'-bipyridine (0.074 g, 0.425 mmol) was added, and the acetone solution was heated at reflux under argon for 20 h. The solution was constantly protected from light. After about 20 h, the condenser was removed and the volume of acetone reduced to ~10 mL. More acetone was added and the volume reduced again. The remaining solution was filtered through a medium glass frit to remove insoluble KPF₆ and added dropwise to stirred anhydrous ethyl ether (~175 mL). The precipitate was collected by suction filtration and dried under vacuum in a desiccator. When dry the product was washed with ~30 mL of water to remove the water-soluble salts and then redried under vacuum and reprecipitated from acetone/ether, yield ~90% for all complexes.

Product purity was ascertained using electrochemistry (the absence of other noticeable redox couples) or by thin layer chromatography. Further purification was accomplished by chromatography on alumina or cellulose using CH₃OH/CH₂Cl₂, CH₃CN/CH₂Cl₂, CH₃OH/C₆H₆, or CH₃CN/C₆H₆ mixtures as eluents, as described above. The dimeric complexes had chromatographic properties like those of the monomers described above but retention times were generally longer than for the monomers. Yields after chromatography were 55–60%. Elemental analysis results are given in Table I.

[(bpy)₂ClRu(BPA)RuCl(bpy)₂](PF₆)₂. **Route B.** [(bpy)₂-Ru(NO)](PF₆)₂ (0.161 g, 0.209 mmol) was dissolved in ~30 mL of acetone and protected from the light. KN₃ (0.017 g, 0.210 mmol) dissolved in a minimum (~5 mL) of CH₃OH was added dropwise to the stirred solution. After ~15 min [(bpy)₂ClRu(BPA)](PF₆) (0.161 g, 0.174 mmol) dissolved in 20 mL of acetone was added and the mixture was allowed to heat at reflux under argon for 20 h. After 20

h, the red-orange solution was slowly filtered through a medium glass frit into stirred anhydrous ether (~175 mL), and the precipitate collected by suction filtration and dried under vacuum in a desiccator, yield 90%. The complex was further purified by chromatography giving a final yield of ~55%.

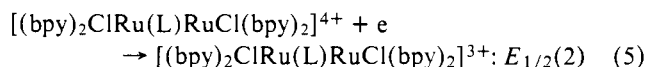
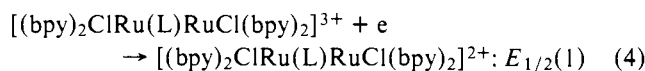
[(bpy)₂ClRu(L)RuCl(bpy)₂](PF₆)₄·2H₂O, (L) = pyr, 4,4'-bpy, and BPE. The oxidized (Ru(III)-Ru(III)) forms of the dimeric complexes were obtained from the reduced species by oxidation using (NH₄)₂Ce(NO₃)₆. The procedure has been described elsewhere.¹¹ In a typical preparation [(bpy)₂ClRu(BPE)RuCl(bpy)₂](PF₆)₂ (0.316 g, 0.225 mmol) was dissolved in ~20 mL of acetone. Tetra-*n*-butylammonium chloride, in excess, dissolved in acetone was added, causing the immediate precipitation of the chloride salt which was collected by suction filtration and washed with three 10-mL portions of acetone. The salt was then dissolved in 0.1 M HCl and (NH₄)₂Ce(NO₃)₆ (a 10% excess) was added. The oxidation is immediate, causing a color change from purple-red to brownish-green. A saturated solution of NH₄PF₆ (15 mL) was then added and the PF₆⁻ salt which precipitates out of solution was collected by suction filtration, washed with 0.1 M HCl, and dried in vacuo. Elemental analyses are given in Table I.

For spectrophotometric work the oxidized complexes were generated in situ using Ce(IV) solutions. The preparation and standardization of these solutions have been described elsewhere.^{18b}

[(bpy)₂ClRu(L)RuCl(bpy)₂]³⁺. The mixed-valence (Ru(II)-Ru(III)) complexes were generated in solution by one-electron oxidation either electrochemically, using Ce(IV), or by mixing equimolar amounts of the reduced (Ru(II)-Ru(II)) and the oxidized (Ru(III)-Ru(III)) dimers in the same solution.

Results

Electrochemistry. Cyclic voltammetry and coulometry experiments in 0.1 M TBAH/CH₃CN vs. SSCE (saturated sodium chloride calomel electrode) at 25 ± 2 °C show that the series of Ru(II)-Ru(II) dimers [(bpy)₂ClRu(L)RuCl(bpy)₂]²⁺ undergo two one-electron oxidations. *E*_{1/2} values (Table II) were calculated from cyclic voltammograms (*E*_{1/2} = (*E*_{p,a} - *E*_{p,c})/2). The *E*_{1/2} values are formally reduction potentials, except for a usually small correction term for differences in diffusion coefficients, and refer to the equations:



Separate values for *E*_{1/2}(1) and *E*_{1/2}(2) are resolved only when L = pyr and pym. For L = 4,4'-bpy, BPE, and BPA only one wave was observed in the potential region from 0 to 1.4 V, but the peak separations are considerably larger than the theoretically predicted 58 mV. The large Δ*E*_p values could result from the close proximity of two closely spaced one-electron waves.¹⁰ Since the current is additive for each process the result would be a slight apparent increase in Δ*E*_p. Variations in scan rate (50–500 mV/s) left peak potentials unaffected and the ratios of anodic to cathodic peak currents

Table II. Electrochemical Data for the Dimer [(bpy)₂ClRu(L)RuCl(bpy)₂]^{3+/2+} and 4+/3+ Couples^a

couple	$E_{1/2}$, V ^b	ΔE_p , mV ^c	n^d
[(bpy) ₂ ClRu(pyr)RuCl(bpy) ₂] ^{3+/2+} ^e	0.89	75	1
[(bpy) ₂ ClRu(pyr)RuCl(bpy) ₂] ^{4+/3+} ^e	1.01	75	1
[(bpy) ₂ ClRu(pym)RuCl(bpy) ₂] ^{3+/2+} ^f	0.87	60	1.3 (at 0.95 V)
[(bpy) ₂ ClRu(pym)RuCl(bpy) ₂] ^{4+/3+} ^f	0.99	60	2.0 (at 1.2 V)
[(bpy) ₂ ClRu(4,4'-bpy)RuCl(bpy) ₂] ^{4+/3+} and 3+/2+	0.82	80	
[(bpy) ₂ ClRu(BPE)RuCl(bpy) ₂] ^{4+/3+} and 3+/2+	0.78	80	1.90
[(bpy) ₂ ClRu(BPA)RuCl(bpy) ₂] ^{4+/3+} and 3+/2+	0.77	90	2.03

^a In 0.1 M [N(*n*-C₄H₉)₄](PF₆)-CH₃CN at room temperature. ^b Vs. the saturated sodium chloride calomel electrode. ^c Calculated from the difference in anodic and cathodic peak potentials. ^d Determined by coulometry. ^e Taken from ref 3a. ^f Taken from ref 17.

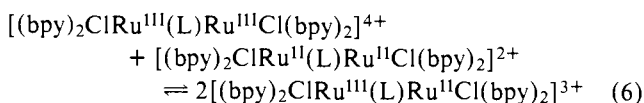
Table III. Electronic Spectra for the Ions [(bpy)₂ClRu(L)RuCl(bpy)₂]^{m+} ($m = 2, 3, 4$) in Acetonitrile

complex	λ_{\max} , nm ^a	$\epsilon \times 10^{-4}$, M ⁻¹ cm ⁻¹ ^b	complex	λ_{\max} , nm ^a	$\epsilon \times 10^{-4}$, M ⁻¹ cm ⁻¹ ^b
[(bpy) ₂ ClRu(pyr)RuCl(bpy) ₂] ²⁺ ^c	513	2.6	[(bpy) ₂ ClRu(pym)RuCl(bpy) ₂] ⁴⁺	425	0.49
	498 (sh)			345	0.91
	339	1.2		313	4.72
	292	9.2		290	4.72
	243	3.8		247	4.63
[(bpy) ₂ ClRu(pym)RuCl(bpy) ₂] ²⁺	482	2.02	[(bpy) ₂ ClRu(4,4'-bpy)RuCl(bpy) ₂] ⁴⁺	420	0.75
	455 (sh)			365 (sh)	
	385 (sh)			313	5.08
	349	1.52		295	6.12
	293	11.2		247	5.89
	255 (sh)			417 (sh)	0.64
[(bpy) ₂ ClRu(4,4'-bpy)RuCl(bpy) ₂] ²⁺	241	4.95	[(bpy) ₂ ClRu(BPE)RuCl(bpy) ₂] ⁴⁺	355 (sh)	
	491	2.77		312	8.22
	465 (sh)			303	7.64
	410	1.80		247	5.35
	368 (sh)			420 (sh)	0.52
[(bpy) ₂ ClRu(BPE)RuCl(bpy) ₂] ²⁺	293	10.6	[(bpy) ₂ ClRu(BPA)RuCl(bpy) ₂] ⁴⁺	350 (sh)	1.26
	260 (sh)			313	6.06
	244	5.74		298	6.44
	496	3.67		248	7.05
	460 (sh)			508	1.4
	428 (sh)	2.27		475 (sh)	
	356	1.62		310 (sh)	
[(bpy) ₂ ClRu(BPA)RuCl(bpy) ₂] ²⁺	294	13.8	[(bpy) ₂ ClRu(pyr)RuCl(bpy) ₂] ³⁺ ^c	292	6.0
	286 (sh)			244	4.1
	256 (sh)			482	1.4 ^d
	243	4.35		450 (sh)	
	503	1.70		343	1.3 ^d
	460 (sh)			313 (sh)	
	357	2.40		293	7.0 ^d
[(bpy) ₂ ClRu(pyr)RuCl(bpy) ₂] ⁴⁺ ^c	298	11.3	[(bpy) ₂ ClRu(4,4'-bpy)RuCl(bpy) ₂] ³⁺	243	3.4 ^d
	285 (sh)			490	1.4 ^d
	248	4.97		420 (sh)	
	430	0.4		315 (sh)	
	310	5.0		298	7.4 ^d
	300	5.0		248	5.9 ^d
	246	4.9		502	1.1 ^d
[(bpy) ₂ ClRu(BPA)RuCl(bpy) ₂] ³⁺			[(bpy) ₂ ClRu(BPA)RuCl(bpy) ₂] ³⁺	356 (sh)	1.9 ^d
				315	1.1 ^d
				297	9.4 ^d
				248	5.4 ^d

^a At room temperature, ± 2 nm in CH₃CN. ^b Estimated error in values is $\pm 10\%$. ^c From ref 3a. ^d Estimated assuming that K for the comproportionation equilibrium in eq 6 is 4.

($i_{p,a}/i_{p,c}$) were ~ 1 for each process. Attempts to resolve the two one-electron processes by potentiometric titrations were also unsuccessful.

Using the $E_{1/2}$ values, the value of K_{com} for the comproportionation equilibrium:



is $\sim 10^2$ for L = pyr and pym in 0.1 M [N(*n*-Bu)₄](PF₆/

CH₃CN. The values appear to be the same in pure acetonitrile from spectrophotometric experiments. Quantitative calculations based on the 3+ mixed-valence dimers where L = pyrimidine or pyrazine have been corrected for the small amounts of the 4+ and 2+ ions present at equilibrium.

Electronic Spectra. The ultraviolet-visible spectra of the series of dimers are all similar. Spectral results for the Ru(II)-Ru(II) dimers, for the mixed-valence 3+ dimers, and for the Ru(III)-Ru(III) 4+ dimers, all in acetonitrile, are summarized in Table III.

The spectra of the 2+ and 4+ dimers are nearly those of

Table IV. Near-Infrared Spectral Data for the Ions $[(bpy)_2ClRu(L)RuCl(bpy)_2]^{3+}$

solvent	$(1/D_{op}) - (1/D_s)$	L = pym		pyr ^a		4,4'-bpy		BPE	
		λ_{max}^b , nm	ν_{max}^c , $cm^{-1} \times 10^{-3}$	λ_{max}^b , nm	ν_{max}^c , $cm^{-1} \times 10^{-3}$	λ_{max}^b , nm	ν_{max}^c , $cm^{-1} \times 10^{-3}$	λ_{max}^b , nm	ν_{max}^c , $cm^{-1} \times 10^{-3}$
acetone	0.493					1010 ± 5	9.90 ± 0.05	920 ± 10	10.87 ± 0.1
acetonitrile	0.526	1360 ± 5	7.34	1300	7.69	985 ± 5	10.15 ± 0.05	925 ± 10	10.81 ± 0.1
N,N-dimethylformamide	0.462					1060 ± 10	943 ± 0.1	930 ± 10	10.75 ± 0.1
dimethyl sulfoxide	0.438			1365	7.33	1060 ± 10	943 ± 0.1	1010 ± 10	9.90 ± 0.1
propylene carbonate	0.481			1335	7.49	1025 ± 5	980 ± 0.04	950 ± 15	10.53 ± 0.2
nitrobenzene	0.384			1400	7.14	1110 ± 10	9.01 ± 0.1	1030 ± 20	9.71 ± 0.2
H ₂ O/D ₂ O ^c	0.546			1270	7.87	890 ± 20	11.24 ± 0.3	830 ± 15	11.90 ± 0.3

^a From ref 3a. ^b ±10 nm. ^c 0.1 M HCl in D₂O for L = 4,4'-bpy, 0.1 M HCl/H₂O for L = BPE.

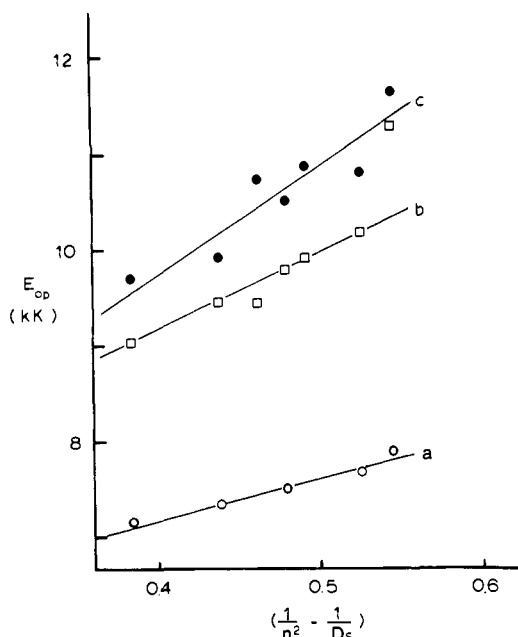


Figure 1. Plots of E_{op} vs. $[(1/D_{op}) - (1/D_s)]$ for the near-IR bands of the mixed-valence dimers $[(bpy)_2ClRu(L)RuCl(bpy)_2]^{3+}$: (a) L = pyr (from ref 3a); (b) L = 4,4'-bpy; (c) L = BPE.

related Ru(II) or Ru(III) complexes, respectively.^{3a,11,18b} The spectra of the mixed-valence ions in the UV-visible spectral region are nearly the sum of the spectra of $[(bpy)_2ClRu^{II}(L)]^+$ and $[(bpy)_2ClRu^{III}(L)]^{2+}$ groups. There are no new or unusual absorption bands in this spectral region for the mixed-valence ions.

Near-Infrared Spectra. In the near-infrared region, new absorption bands appear for the mixed-valence ions which are not present for either the 2+ or 4+ dimeric ions. The near-infrared spectra of the mixed-valence complexes $[(bpy)_2ClRu(L)RuCl(bpy)_2]^{3+}$ in which L = pyr,^{3a} pym,¹⁷ 4,4'-bpy, and BPE were obtained in a variety of solvents and the results are summarized in Table IV where values of λ_{max} and ν_{max} , the energy of the absorption at λ_{max} , as well as values of the quantity $(1/D_{op} - 1/D_s)$ for each solvent are also given. D_s and D_{op} are the static and optical dielectric constants of the solvents used. The near-IR bands for all the complexes are broad and $\Delta\bar{\nu}_{1/2}$, the bandwidth at half-height, is on the order of 4000–6000 cm^{-1} . In general, bandwidths were determined by doubling the half-bandwidths on the high-energy side because of tailing at low energies into regions of solvent IR overtone absorptions. In all cases, in the series of solvents used the ratios of the experimental values for $\Delta\bar{\nu}_{1/2}$ to the values calculated from eq 7 were in the range 1.1–1.4.

$$\bar{\nu}_{max} = (\Delta\bar{\nu}_{1/2})^2 / 2.31 \quad (\bar{\nu}_{max} \text{ and } \Delta\bar{\nu}_{1/2} \text{ in } cm^{-1}) \quad (7)$$

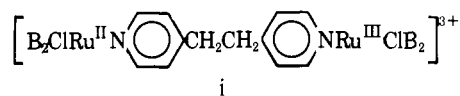
Equation 7 has been derived by Hush for IT bands. The larger

than predicted bandwidths are not unexpected given the single oscillator model used by Hush in deriving eq 7.

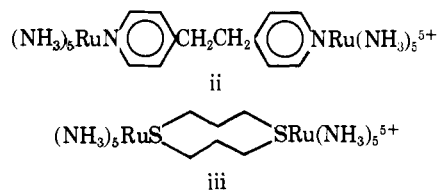
Solvent Dependence of Near-IR Bands. In Figure 1 are shown plots of E_{op} vs. $(1/D_{op} - 1/D_s)$ in the solvents used for the IT bands of the dimers $[(bpy)_2ClRu(L)RuCl(bpy)_2]^{3+}$ (L = pyr,^{3a} 4,4'-bpy, and BPE). A linear least-squares program was used to fit the data and the lines drawn represent the best fit straight lines. The slopes, y intercepts, and correlation coefficients for the three plots shown in Figure 1 are given in Table V as are values of λ_i and λ_o , and d , the internuclear distance between redox sites. The significance of all of these terms will be discussed in detail in later sections.

The uncertainty in the ϵ_{max} values in Table V for the 4,4'-bpy and BPE dimers arises because K_{com} values for the comproportionation equilibria in eq 6 are unknown. The high values in Table V were calculated assuming $K_{com} = 4$ and the low values that K_{com} is sufficiently large that only the mixed-valence ions are present in appreciable concentrations.

Attempts to observe IT bands for the dimer i were un-



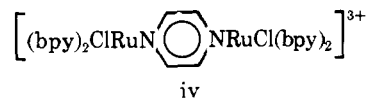
successful, which is not surprising given the saturated region in the bridging ligand. However, it should be noted that evidence for very weak IT bands has been found for the ions ii²¹ and iii²²



and studies on the BPA dimer at high dimer concentrations might show the existence of a weak IT band.


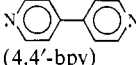
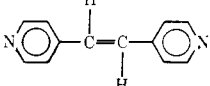
Discussion

The evidence for localized valences and weak electronic coupling in the dimer iv has been presented elsewhere.^{3a} For



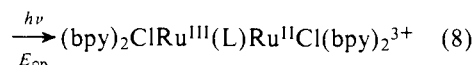
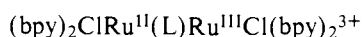
the other mixed-valence dimers, the longer Ru–Ru separation and/or the higher energy of π^* levels in the bridging ligands are expected to lead to even smaller electronic interactions between the Ru(II) and Ru(III) sites.^{18,20} The properties of the dimers are consistent with this prediction as shown by the weakness in intensity of the IT bands and by the clear similarities in optical spectra and redox potentials for the mixed-valence dimers with isolated monomeric complexes of Ru(III) and Ru(II) which are related chemically. For the mixed-valence dimers, the relatively weak near-IR bands can then be assigned to metal–metal charge transfer (MMCT) or inter-

Table V. Experimental and Calculated Results from Plots of E_{op} vs. $[(1/D_{op}) - (1/D_s)]$ for the Near-IR Bands of the Dimers $[(bpy)_2ClRu(L)RuCl(bpy)_2]^{3+}$

L	slope (obsd), V	y int, V	correlation coefficient <i>r</i>	λ_i , V	λ_o , ^a V	<i>d</i> , Å	ϵ_{max} , ^a M ⁻¹ cm ⁻¹
 (pyr)	0.537 ^b	0.676 ^b	0.99 ^b	0.71	0.29	6.9	455 ^b at 7.69×10^3 cm ⁻¹
 (4,4'-bpy)	0.980 ^c	0.744 ^c	1.00 ^c	0.78	0.54	11.1	100–200 at 10.15×10^3 cm ⁻¹
 (BPE)	1.34	0.674	0.92	0.70	0.70	13.2	135–270 at 10.81×10^3 cm ⁻¹

^a Values in CH₃CN. ^b From ref 3a. ^c Calculated excluding the value in 0.1 M HCl/D₂O.

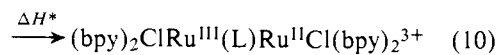
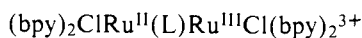
valence transfer (IT) bands (eq 1 and 8). The assignment is consistent with the observed bandwidths and, as discussed below, with the dependence of the band energies both on solvent properties and on the distance separating the redox sites.



Role of the Medium. In a localized mixed-valence ion, the excess electron is essentially trapped on one site. The trapping occurs because the bond distances and structure at the chemical sites are dependent on electron content and vary with oxidation state. The net effect is to create a vibrational trapping energy. If the inner- and outer-sphere contributions to the vibrational trapping energy are separable, the energy of the IT band is given by

$$E_{op} = \chi_i + \chi_o = \chi \quad (9)$$

χ_i and χ_o are the inner- and outer-sphere internal energy contributions to the optical barrier to electron transfer. Assuming a harmonic oscillator model for the vibrations in the classical limit and also that electronic coupling between the redox sites is weak, E_{op} is related to the energy or heat of activation for the related thermal process



by

$$\Delta H^* = E_{op}/4 = \chi/4 \quad (11)$$

For an intramolecular reaction like eq 10 where $\Delta G = 0$, χ_i and χ_o are essentially equal to the corresponding free-energy terms λ_i and λ_o .^{26,28}

The inner- and outer-sphere vibrational contributions to the thermal barrier to electron transfer have been treated quantum mechanically by a number of authors^{23–25} and classically by Marcus²⁶ and Hush.²⁷ In the high-temperature limit where the vibrational spacings involved are small compared to $k_B T$ ($\hbar\omega_n \ll k_B T$), the quantum-mechanical treatment leads to the classical result.^{23,24}

For optical electron transfer, the effect of solvent polarization has been treated in terms of a dielectric continuum model:^{2a,29,30}

$$\lambda_o = 1/2 \left(\frac{1}{D_{op}} - \frac{1}{D_s} \right) \int (\bar{\mathbf{D}}_f - \bar{\mathbf{D}}_i)^2 dV \quad (12)$$

Equation 12 is an expression for the free-energy difference before and after electron transfer arising from solvent polarization effects. $\bar{\mathbf{D}}_f$ and $\bar{\mathbf{D}}_i$ are the dielectric displacement vectors associated with the charge distributions in the final and initial states. D_s and D_{op} are the optical and static dielectric constants of the medium. The integration is performed from the surface of an inner volume described by the metal plus inner coordination sphere ligands throughout the outer volume surrounding the ion.

The choice of the dielectric constants in eq 12 follows from the nature of the optical electron transfer process. The use of D_{op} for the medium after electron transfer has occurred is appropriate from the “frozen nuclei” approximation of the Franck–Condon principle. Since the time scale for the optical transition is short compared to the time for transitions between vibrational levels, only the electronic polarization component of D_s can respond to the electron transfer. The orientational and atomic displacement contributions to D_s which are vibrational in nature are too slow to respond.

Problems exist in the selection of an appropriate value for D_s . With high charge densities at the redox sites, dielectric saturation effects are important.^{31,32} With ligands like NH₃, H₂O, or CN⁻, hydrogen bonding with solvent can strongly influence solvent properties close to the ions.³³ In solutions containing high concentrations of electrolytes, the contribution of the electrolyte to the polarization properties of the medium must be taken into account.^{34,35} If there are low-frequency medium modes which are slow on the thermal electron transfer time scale, they will not contribute to D_s .

However, for the complexes described here, the redox sites are large and charge densities low. Given the ligands involved, there should be no complications from hydrogen bonding. Most of the optical experiments were carried out in dilute solutions with no added electrolyte. Perhaps of most importance is the fact that for the polar solvents used here D_s is large compared to D_{op} . The medium dependence in eq 12 is dominated by the term inverse in the electronic polarization of the medium and variations in the static polarization are numerically small.

For the case of two charged spheres of radii a_1 and a_2 either separated by an internuclear distance d or in close contact ($d = a_1 + a_2$), eq 12 can be integrated to give

$$\lambda_o = e^2 \left(\frac{1}{2a_1} + \frac{1}{2a_2} - \frac{1}{d} \right) \left(\frac{1}{D_{op}} - \frac{1}{D_s} \right) \quad (13)$$

Since for a chemically symmetric mixed-valence ion $a_1 \approx a_2$, eq 13 becomes

$$\lambda_o = e^2 \left(\frac{1}{a_1} - \frac{1}{d} \right) \left(\frac{1}{D_{op}} - \frac{1}{D_s} \right) \quad (14)$$

Table VI. Data for the Dependence of E_{op} on d in Selected Solvents for the Mixed-Valence Dimers $[(bpy)_2ClRu(L)RuCl(bpy)_2]^{3+}$

L	$d, \text{\AA}$	$a_1, \text{\AA}$	$E_{op}, \text{cm}^{-1} \times 10^{-3}$			
			CH_3CN	nitrobenzene	propylene carbonate	Me_2SO
pym	6.0	5.9	7.36			
pyr	6.9	6.0	7.69	7.14	7.49	7.33
4,4'-bpy	11.1	6.4	10.15	9.01	9.80	9.43
BPE	13.2	6.5	10.81	9.71	10.53	9.90
			From Plots of E_{op} vs. $1/d$			
y intercept, $\text{cm}^{-1} \times 10^{-3}$			13.6	12.6	14.1	13.0
slope, $\text{cm}^{-1} \times 10^{-3}/\text{\AA}$			-38.8	-39.4	-47.2	-40.6

Hush²⁷ has derived the equation

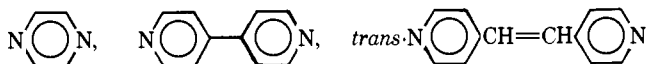
$$\lambda_o/4 = \frac{e^2}{4} \left(\frac{1}{2a_1} + \frac{1}{2a_2} - \frac{1}{d} \right) \left(\frac{1}{D_{op}} - \frac{1}{D_s} \right)$$

for thermal electron transfer using a thermochemical approach. From his analysis, the terms in eq 13 can be interpreted as follows: (1) The terms $e^2(1/2a)((1/D_{op}) - (1/D_s))$ are differences in solvation energies for the two redox sites in media having dielectric constants D_{op} and D_s . (2) The term $(e^2/d) \cdot (1/D_s)$ arises because of a change in electrostatic repulsion or attraction between the redox sites. (3) The term $(e^2/d)(1/D_{op})$ accounts for the electrostatic interaction between the excited electron-electron hole pair.

The integrated form in eq 13 is not exact since it fails to account for the volume of the ions, but the correction involved appears to be small.^{36,37} Of a more serious consequence is the fact that, for three of the four mixed-valence ions, L = pym, pyr, and 4,4'-bpy, the integrated result cited in eq 13 is inappropriate. For those ions the internuclear distance is less than the sum of the radii and the boundary condition $d \geq a_1 + a_2$ is not met. The coordination spheres describing the redox sites interpenetrate rather than being in close contact.

For the mixed-valence ions, the redox sites are not spherical. Average molecular radii are shown in Table VI. They were obtained by averaging the four distances along the Ru-N(bpy) axes from the ruthenium ion to the end of the van der Waals radii of the remote hydrogen atoms (7.1 Å), the ruthenium to chlorine (2.40 Å)³⁸ plus van der Waals radius (1.80 Å),³⁹ and half the Ru-Ru distance. In the calculations an average Ru-N bond distance of 2.12 Å was used⁴⁰ and the dimensions of the bipyridyl ligands were taken from crystal structures of the related complexes $\text{Fe}(\text{phen})_3^{2+}$,^{41a} $\text{Fe}(\text{phen})_3^{3+}$,^{41b} and $\text{Cr}(\text{bpy})_3^{0/+}$.^{41c} The Ru-Ru distances were calculated from standard C-C and C-N bond distances and a Ru-N distance of 2.12 Å.

Even though the integrated geometrical term in eq 13 does not properly describe the series of mixed-valence dimers, it is possible to test the influence of the medium by observing how the energies of the IT absorption bands vary in a series of solvents.⁵ For the three ions where L =



the predicted dependence of E_{op} on $(1/D_{op}) - (1/D_s)$ is observed as shown by the plots in Figure 1 and by the correlation coefficients in Table V.

From eq 9 the inner-sphere and outer-sphere contributions to E_{op} are separable. Since $\chi_o \sim \lambda_o$ and since λ_o is given by eq 14, it follows that

$$E_{op} = \lambda_i + e^2 \left(\frac{1}{a_1} - \frac{1}{d} \right) \left(\frac{1}{D_{op}} - \frac{1}{D_s} \right) \quad (15)$$

Equation 15 predicts that extrapolation of the solvent dependence plots in Figure 1 to the intercept should give numerical values for λ_i . The value at the intercept corresponds experi-

mentally to the measurement of E_{op} in a nonpolar solvent where $D_{op} = D_s$.

In fact, the extrapolations give the sum of all contributions to E_{op} which are insensitive to changes in the medium. The mixed-valence dimers contain spin-paired $d^6(\text{Ru(II)})$ and $d^5(\text{Ru(III)})$. Because of the low symmetries at the redox sites the $d\pi$ levels are probably nondegenerate. If the dominant contribution to the electronic transition occurs because of excitation from a Ru(II) level other than the highest level, there could be an additional factor in E_{op} whose magnitude would depend on zero-field splitting and spin-orbit coupling. This point was made recently by Creutz.⁴² Such a situation is perfectly reasonable given the differences in electronic orbital overlap factors expected for the various donor-acceptor orbital combinations. The lack of obvious structure for the Gaussian-shaped IT bands^{1,3} suggests that either a single donor-acceptor orbital pair dominates the transition or that, if there are multiple orbital contributions, the energy spacings between levels are small compared to the observed bandwidths.

Values for λ_i obtained by extrapolation are given in Table V. In a proper accounting of the role of inner-sphere vibrations the relevant modes must be considered and treated quantum mechanically since, in general, the vibrational spacings are not small compared to $k_B T$. The necessary vibrational information is not yet available for the mixed-valence dimers, but the numerical values for λ_i in Table V are revealing. They show that, within experimental error, the inner-sphere vibrational contributions to E_{op} are the same for the three mixed-valence ions. The lack of a dependence of λ_i on the bridging ligand is expected given the chemical similarity in the bridging ligands and the weak electronic coupling between redox sites. The two redox sites act as uncoupled oscillators in terms of the inner-sphere vibrations. However, the outer-sphere or solvent vibrations are coupled to both of the redox sites and that coupling is the origin of the $e^2(1/d)((1/D_{op}) - (1/D_s))$ term in eq 13.

The magnitude of λ_i is surprising given the lack of significant differences in metal-ligand bond distances in pairs of ions like $\text{Ru}(\text{NH}_3)_6^{3+}$ and $\text{Ru}(\text{NH}_3)_6^{2+}$ ⁴⁰ and $\text{Fe}(\text{phen})_3^{3+}$ and $\text{Fe}(\text{phen})_3^{2+}$.^{41a,b} Although not much can be said in the absence of detailed vibrational and structural information, it may be worth noting that there could be significant changes in Ru-Cl bond distances with oxidation state and noting again that the λ_i values may include an electronic contribution arising from nondegeneracies in the donor and acceptor $d\pi$ levels.

A similar observation has been made by Endicott and co-workers in their crystallographic studies on Co(II) and Co(III) macrocyclic complexes.⁴³ Using measured bond distances, their estimates for calculated $\lambda_i/4$ values using a classical model for the vibrations seem to be consistently too low.

Role of Interreactant Distance. In comparing the data in Figure 1 and Tables IV-VI for the four mixed-valence ions, it is clear that the energies of the optical transitions increase in magnitude as the distance between redox sites increases. Since λ_i is independent of d , the origin of the effect must be in

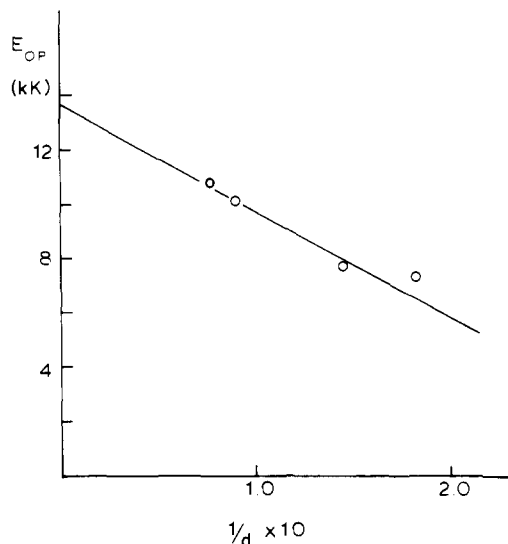


Figure 2. Plot of E_{op} vs. $1/d$ for the mixed-valence dimers $[(bpy)_2Cl-Ru(L)RuCl(bpy)_2]^{3+}$ ($L = \text{pym, pyr, 4,4'-bpy, BPE}$) in acetonitrile.

the solvent polarization term. The dielectric continuum result (eq 13–15) predicts a $-1/d$ dependence for E_{op} which can be seen more clearly in eq 16, which was obtained by rearranging eq 15.

$$E_{op} = \left[\lambda_i + \frac{e^2}{a_1} \left(\frac{1}{D_{op}} - \frac{1}{D_s} \right) \right] - \frac{e^2}{d} \left(\frac{1}{D_{op}} - \frac{1}{D_s} \right) \quad (16)$$

In Figure 2 is shown a plot of E_{op} vs. $1/d$ for the four mixed-valence ions in acetonitrile including the case where $L = \text{pyrimidine}$. In Table VI are summarized slope and intercept data obtained from similar plots of E_{op} vs. $1/d$ for the three ions where $L = \text{pyr, 4,4'-bpy, and BPE}$ in a series of polar solvents.

Although the linear decrease in E_{op} with $1/d$ predicted by eq 16 is observed, quantitative agreement between experiment and theory is not satisfactory. Using an average value of $\lambda_i = 0.73 \text{ V}$ taken from Table V and $a_1 = 6.4 \text{ \AA}$ gives as a theoretical equation for the data, $E_{op} (\text{V}) = 1.91 - (7.57/d)$. An estimation of the best fit of the data in Figure 2 to a straight line gives an equation of the form $E_{op} (\text{V}) = 1.68 - (4.81/d)$. The lack of agreement with theory is not unexpected since, as noted above, the boundary conditions used to obtain eq 13–16 are unrealistic for three of the four mixed-valence ions.

Using the data for the IT absorption bands, it is possible to derive an equation for E_{op} empirically which is of the same form as eq 16. In the modified equation (eq 17), λ_i and the properties of the medium are kept unchanged, but it is assumed that the values for d calculated on the basis of molecular structure are inappropriate.

$$E_{op} = \lambda_i + e^2 \left(\frac{1}{a_1} - \frac{1}{d'} \right) \left(\frac{1}{D_{op}} - \frac{1}{D_s} \right) \quad (17)$$

In eq 17 $d' = d + \Delta d$ is taken to be a variable parameter equal to the actual distance between redox sites plus an increment Δd . Using $\lambda_i = 0.73 \text{ V}$ and the dielectric constants appropriate to acetonitrile, eq 17 becomes

$$E_{op} (\text{V}) = 0.73 + 7.57 \left(\frac{1}{a_2} - \frac{1}{d'} \right) \quad (18)$$

For the four mixed-valence ions, eq 18 can be solved for d' ($=d + \Delta d$) and, using the experimental values for E_{op} in acetonitrile, Δd is found to be 0.8 \AA for $L = \text{pyrimidine}$ and 0.4 \AA for the other three ions, giving an average value of $\Delta d = 0.5 \text{ \AA}$.

In Figure 3 is shown a plot of the experimental E_{op} values vs. $((1/a_1) - (1/(d + 0.5)))$. The straight line is the theoretical line calculated using eq 18 where $d' = d + 0.5 (\text{\AA})$. The good

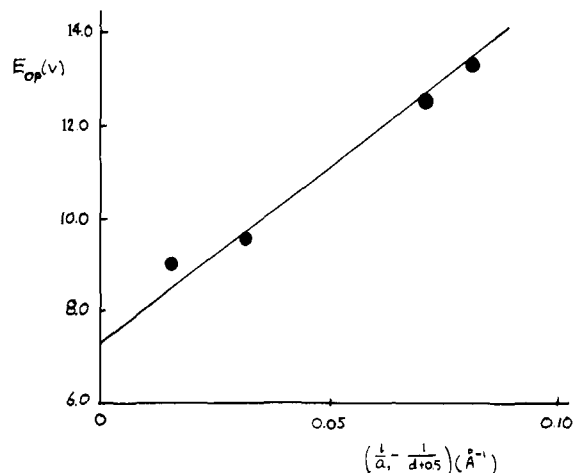


Figure 3. Plot of E_{op} vs. $((1/a_1) - (1/(d + 0.5)))$ for the mixed-valence ions $[(bpy)_2Cl-Ru(L)RuCl(bpy)_2]^{3+}$ in acetonitrile.

agreement between experiment and theory shows that, at least for the series of mixed-valence ions studied here, a simple empirical correction to the prediction made by dielectric continuum theory satisfactorily accounts for the effect of solvent polarization on the energy of the optical transition. The form of the correction is appropriate, at least qualitatively, since, as d becomes less than $2a_1$, electron transfer occurs as an "embedded" process within the material of the dimer itself. The solvent occupies an increasingly remote outer volume and interactions with its polarization properties are overestimated by a simple $1/d$ dependence.

Cannon has proposed a more realistic approach to the integration of eq 12 for cases like the mixed-valence dimers.³⁶ His approach is based on the earlier work of Kirkwood and Westheimer on solvation energies for ellipsoidal shapes,⁴⁵ and the reader is referred to his papers and to the recent paper by German for a more detailed discussion.^{36c}

There is another point of interest in the context of the distance dependence effect which relates directly to the observations made here. Brown and Sutin have shown recently that, for a series of closely related outer-sphere reactions where $d > a_1 + a_2$, the expected dependence on $1/d$ is observed.⁴⁴

Another test of the empirically modified dielectric continuum equation is available by comparing calculated and experimental slopes for the data. In Figure 1, E_{op} is shown plotted against $((1/D_s) - (1/D_{op}))$. From eq 15 the theoretical slopes are given by $e^2((1/a_1) - (1/d))$ or, using the empirical correction in eq 18 where $d' = d + 0.5$, by $e^2((1/a_1) - (1/d'))$. Theoretical and experimental values for the slopes of the solvent plots are compared in Table VII. Once again, the agreement between experiment and theory is striking and shows that a continuum model for the dimers studied here, based on a relatively simple approximation to molecular shape, is adequate to account for solvent polarization effects.

Role of Distance between Redox Sites in Outer-Sphere Reactions. In an outer-sphere reaction, an initial diffusion together of the reactants occurs followed by electron transfer:

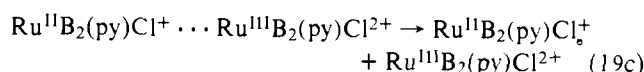
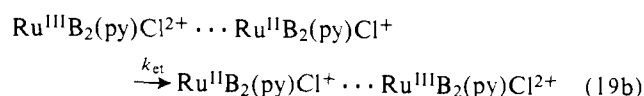
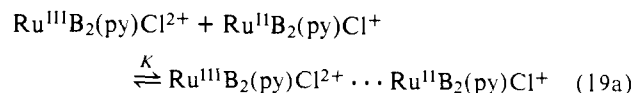
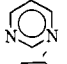
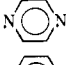
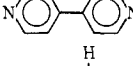
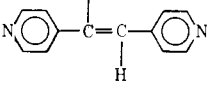


Table VII. Calculated and Experimental Slopes for the Variation in E_{op} with $((1/D_{op}) - (1/D_s))$ for the Mixed-Valence Ions $[(bpy)_2ClRu^{II}(L)Ru^{III}Cl(bpy)_2]^{3+}$

L	$d, \text{\AA}$	$a_1, \text{\AA}$	exptl slope, V	calcd ^a slope, V
	6.1	5.9		
	6.9	6.0	0.54	0.45
	11.1	6.4	0.98	1.02
	13.2	6.5	1.34	1.16

^a Calculated from $e^2((1/a_1) - (1/(d + 0.5)))$. Note eq 18.

It is usually assumed that the reactants approach to a close contact distance to form an ion-pair or association complex. At first glance, the assumption of close contact seems surprising at least for like-charged ions where electrostatic repulsion is important. In fact, the distance between redox sites is a variable and the possible role of long-range electron transfer in outer-sphere reactions has been discussed.⁴⁶⁻⁴⁸

The rate constant for outer-sphere electron transfer (eq 19a and 19b) is given by

$$k = k_{et}K_A = \nu_{et} \exp[-(\Delta G_A + \Delta G^*)/RT] \quad (20)$$

$$\ln k = \ln \nu_{et} - \left(\frac{\Delta G_A + \Delta G^*}{RT} \right) \quad (20a)$$

which is of the same form as for intramolecular electron transfer (eq 2), $k = \nu_{et} \exp[-(\Delta G^*/RT)]$, except that the term $K_A = \exp[-(\Delta G_A/RT)]$ has been included to account for the association step. For the $Ru(bpy)_2(py)Cl^{2+/+}$ self-exchange reaction in eq 19a and 19b, the results obtained for the chemically related mixed-valence ions $[(bpy)_2ClRu(L)-RuCl(bpy)_2]^{3+}$ allow the way the energy barrier to electron transfer varies with distance to be evaluated quantitatively.

From eq 11 and 16, ΔG^* ($\Delta S^* \sim 0$)^{26,28} varies with d as

$$\Delta G^* = \left[\frac{\lambda_i}{4} + \frac{e^2}{4a_1} \left(\frac{1}{D_{op}} - \frac{1}{D_s} \right) \right] - \frac{e^2}{4d} \left(\frac{1}{D_{op}} - \frac{1}{D_s} \right) \quad (21)$$

Using the Eigen-Fuoss equation for the ion association step gives for K_A

$$K_A = \frac{4\pi N_0 d^3}{3000} \exp \left[- \left[\frac{Z_A Z_B e^2}{D_s d R T} \left(\frac{1}{1 + \kappa d} \right) \right] \right] \quad (22)$$

and for the corresponding free-energy change

$$\Delta G_A = -RT \ln \frac{4\pi N_0 d^3}{3000} + \frac{Z_A Z_B e^2}{D_s d} \left(\frac{1}{1 + \kappa d} \right) \quad (23)$$

In eq 22 and 23, Z_A and Z_B are the charges on the ions and κ is the Debye-Hückel term $(8\pi N_0 e^2 I / 1000 D_s k_B T)^{1/2}$. N_0 is Avogadro's number and I is the ionic strength. The use of d rather than d' in eq 21 is appropriate assuming that there is no interpenetration of coordination spheres for the outer-sphere reaction.

Combining eq 21 and 23 gives for the sum $\Delta G_A + \Delta G^*$

$$\Delta G_A + \Delta G^* = \left[\frac{\lambda_i}{4} + \frac{e^2}{4a_1} \left(\frac{1}{D_{op}} - \frac{1}{D_s} \right) - RT \ln \frac{4\pi N_0}{3000} \right] - 3RT \ln d - \frac{e^2}{d} \left[\frac{1}{4} \left(\frac{1}{D_{op}} - \frac{1}{D_s} \right) - \frac{Z_A Z_B}{D_s} \left(\frac{1}{1 + \kappa d} \right) \right] \quad (24)$$

Using numerical values appropriate for the $Ru(bpy)_2(py)Cl^{2+/+}$ self-exchange reaction in acetonitrile of λ_i (0.73 V), a_1 (6.6 Å), Z_A (+2), and Z_B (+1) gives for the theoretical

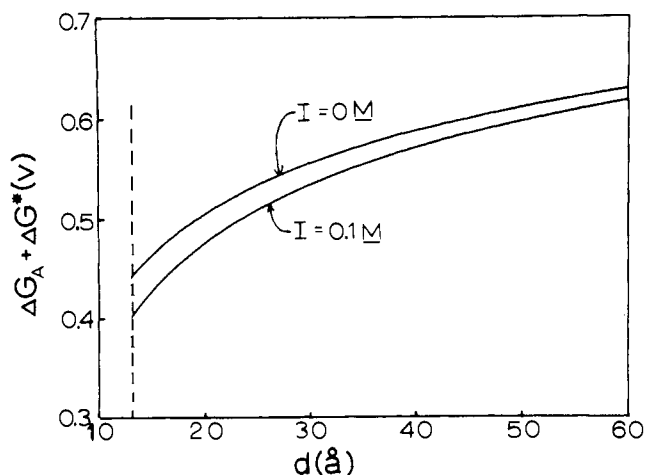


Figure 4. Plots of $\Delta G_A + \Delta G^*$ vs. d calculated from eq 24 and 25 for the outer-sphere exchange reaction between $Ru(bpy)_2(py)Cl^+$ and $Ru(bpy)_2(py)Cl^{2+}$ in acetonitrile under two conditions: $I = 0$ and $I = 0.1$ M.

dependence of the activation barrier on distance

$$\Delta G_A + \Delta G^* = 0.32 + \left(0.08 \ln d - \frac{1.10}{d} \right) \quad (V) \quad (25)$$

Equation 25 gives $\Delta G_A + \Delta G^*$ in V when d is in Å for the ideal, dilute solution case in acetonitrile where $I \sim 0$.

In Figure 4 is shown a plot of the variation of $\Delta G_A + \Delta G^*$ with distance as predicted by eq 25. The striking point about the plot is that, contrary to what has often been assumed, close contact, even between like-charged ions, is favored energetically in polar solvents. The origin of the effect is in the $1/d$ term in eq 24 and 25 which dominates the distance dependence. Both the electrostatic repulsion ($Z_A Z_B e^2 / D_s d$) and $\lambda_o(e^2 / 4d)((1/D_{op}) - (1/D_s))$ terms vary inversely with d but with different signs. In polar solvents where $D_{op} \ll D_s$ and the product $Z_A Z_B$ is sufficiently small, the decrease in λ_o as distance decreases is the more important term and electron transfer when the ions are in close contact is favored energetically. As shown in Figure 4, the effect is accentuated in solutions where added electrolyte decreases electrostatic repulsions by the screening effect of the added ions.

In order to include the complete dependence of the electron transfer rate constant on distance, the distance dependence of the frequency factor for electron transfer, ν_{et} , must also be considered (eq 19b). For cases where electronic coupling is weak, ν_{et} varies with the square of the electron exchange matrix element which arises from overlap between appropriate electronic wave functions at the electron donor and acceptor sites.^{4,23-25} Since wave functions fall off essentially exponentially with distance, the magnitude of ν_{et} will also increase with decreasing d and *there is no basis for expecting that long-range electron transfer should occur for an outer-sphere reaction in polar solvents.*

Final Comments. The results obtained here suggest that a relatively simple dielectric continuum model is adequate for treating the effect of solvent polarization on optical and thermal electron transfer processes in solution. In full detail, the results are probably only valid in polar, nonviscous solvents. In polymers, thin films, or membranes, where D_{op} and D_s are of the same order of magnitude, local inhomogeneities, the existence of low-frequency torsional modes, and other local effects make a proper treatment of the role of the medium far more difficult.

The conclusions reached concerning long-range electron transfer clearly only apply to outer-sphere reactions where the distance between redox sites is a variable. For enzymic sites in a membrane, for different redox sites in frozen solutions or

crystals, long-range electron transfer can be forced to occur. For such reactions an important contribution to the observed rate constant could become a small value of ν_{et} because of a small magnitude for the extent of electronic orbital overlap between donor and acceptor sites.

Assuming that the medium dependence observed here has at least a qualitative predictability for other reactions, some important conclusions can be reached concerning the effects of molecular structure and of medium properties on rates of electron transfer. It follows from eq 13–16 that in order to minimize the λ_0 contribution to the barrier to electron transfer the reactants should be as large as possible ($1/a_1$ in eq 13) and as close together as possible ($1/d$), and the medium should be as nonpolar as possible ($D_s \rightarrow D_{op}$). It is interesting to note that two of these three criteria (size and polarity of the medium) are probably met in most biological membrane electron transfer processes and that for these reactions the trapping effect of the surrounding medium is probably small.

Acknowledgments are made to the Army Research Office—Durham under Grant DAAG29-76-G-0135 and to NIH under Grant 5-R01-GM15238-11 for support of this research.

References and Notes

- (1) Taken in part from: Powers, M. J. Ph.D. Dissertation, The University of North Carolina, Chapel Hill, N.C., 1977.
- (2) (a) Hush, N. S. *Prog. Inorg. Chem.* **1967**, *8*, 391. *Electrochim. Acta* **1968**, *13*, 1005. *Chem. Phys.* **1975**, *10*, 361. (b) Robin, M. B.; Day, P. *Adv. Inorg. Chem. Radiochem.* **1967**, *10*, 247. (c) Meyer, T. J. *Acc. Chem. Res.* **1978**, *11*, 94.
- (3) (a) Callahan, R. W.; Keene, F. R.; Meyer, T. J.; Salmon, D. J. *J. Am. Chem. Soc.* **1977**, *99*, 1064. (b) Callahan, R. W.; Meyer, T. J. *Chem. Phys. Lett.* **1976**, *39*, 82.
- (4) Hopfield, J. J. *Proc. Natl. Acad. Sci. U.S.A.* **1974**, *71*, 3640. *Biophys. J.* **1977**, *18*, 311.
- (5) Tom, G. M.; Creutz, C.; Taube, H. *J. Am. Chem. Soc.* **1974**, *96*, 7827.
- (6) Powers, M. J.; Meyer, T. J. *J. Am. Chem. Soc.* **1978**, *100*, 4393.
- (7) Sullivan, B. P.; Meyer, T. J., *Inorg. Chem.*, in press.
- (8) Powers, M. J.; Salmon, D. J.; Callahan, R. W.; Meyer, T. J. *J. Am. Chem. Soc.* **1976**, *98*, 6731.
- (9) Meyer, T. J., *Chem. Phys. Lett.*, **1979**, *64*, 417.
- (10) Brown, G. M. Ph.D. Dissertation, The University of North Carolina, Chapel Hill, N.C., 1974.
- (11) Callahan, R. W.; Brown, G. M.; Meyer, T. J. *Inorg. Chem.* **1975**, *14*, 1443.
- (12) Sawyer, D. T.; Roberts, J. L., Jr. "Experimental Electrochemistry for Chemists"; Wiley: New York, 1974; pp 203–210.
- (13) Weissberger, A., Ed. "Technique of Organic Chemistry", Vol. VII; Interscience: New York, 1955.
- (14) Sullivan, B. P.; Salmon, D. J.; Meyer, T. J. *Inorg. Chem.* **1978**, *17*, 3334.
- (15) Goodwin, J. B.; Meyer, T. J. *Inorg. Chem.* **1971**, *10*, 471.
- (16) (a) Adeyemi, S. A.; Johnson, E. C.; Miller, F. J.; Meyer, T. J. *Inorg. Chem.* **1973**, *12*, 2371. (b) Adeyemi, S. A.; Braddock, J. N.; Brown, G. M.; Miller, F. J.; Meyer, T. J. *J. Am. Chem. Soc.* **1972**, *94*, 300.
- (17) Powers, M. J.; Meyer, T. J. *Inorg. Chem.* **1978**, *17*, 2955.
- (18) (a) Johnson, E. C. Ph.D. Dissertation, The University of North Carolina, Chapel Hill, N.C., 1975. (b) Callahan, R. W. Ph.D. Dissertation, The University of North Carolina, Chapel Hill, N.C., 1975.
- (19) Murray, R. W.; Reilley, C. N. "Electroanalytical Principles"; Interscience: New York, 1964; p 2175.
- (20) Johnson, E. C.; Callahan, R. W.; Eckberg, R. P.; Hatfield, W. E.; Meyer, T. J. *Inorg. Chem.*, **1979**, *18*, 618.
- (21) Rieder, K.; Taube, H. *J. Am. Chem. Soc.* **1977**, *99*, 7891.
- (22) Stein, C. A.; Taube, H. *J. Am. Chem. Soc.* **1978**, *100*, 1635.
- (23) (a) Kestner, N. R.; Logan, J.; Jortner, J. *J. Phys. Chem.* **1974**, *78*, 2148. (b) Ulstrup, J.; Jortner, J. *J. Chem. Phys.* **1975**, *63*, 4358. (c) Jortner, J. *ibid.* **1976**, *64*, 4860. (d) Fischer, S. F.; Van Duyne, R. P. *Chem. Phys.* **1977**, *26*, 9. (e) Efrima, S.; Bixon, M. *Ber. Bunsenges. Phys. Chem.* **1973**, *77*, 991.
- (24) Duke, C. B. "Proceedings of the Conference on Tunneling in Biological Systems", Chance B., Ed.; in press. Soules, T. F.; Duke, C. B. *Phys. Rev. B* **1971**, *3*, 262.
- (25) Schmidt, P. P. *Spec. Period. Rep.: Electrochem.* **1975**, *5* (Chapter 2); 6 (Chapter 4), and references cited therein.
- (26) Marcus, R. A. *J. Chem. Phys.* **1956**, *24*, 966; **1965**, *43*, 697. Marcus, R. A.; Sutin, N. *Inorg. Chem.* **1975**, *14*, 213, and references cited therein.
- (27) Hush, N. S. *Trans. Faraday Soc.* **1961**, *57*, 557.
- (28) (a) Waisman, E.; Worry, G.; Marcus, R. A. *J. Electroanal. Chem.* **1977**, *82*, 9. (b) Walsh, J.; Meyer, T. J. *Inorg. Chem.*, in press.
- (29) Kubo, R.; Toyozawa, Y. *Prog. Theor. Phys.* **1955**, *13*, 160. Huang, K.; Rhys, A. *Proc. R. Soc. London, Ser. A* **1950**, *204*, 406.
- (30) (a) Levich, V. G. In "Physical Chemistry: An Advanced Treatise", Eyring, H.; Henderson, D.; Jost, W., Eds.; Academic Press: New York, 1970; Vol. 9B. (b) Dogonadze, R. R. In "Reactions of Molecules at Electrodes", Hush, N. S., Ed.; Wiley-Interscience: New York, 1971.
- (31) Beveridge, D. L.; Schnuelle, G. W. *J. Phys. Chem.* **1975**, *79*, 2562, 2566.
- (32) Abraham, M. H.; Liszi, J. *J. Chem. Soc., Faraday Trans. 1* **1978**, 1604.
- (33) Curtis, J.; Sullivan, P., work in progress.
- (34) Davies, M., Senior Reporter. "Dielectric and Related Molecular Processes", Vol. 1; Chemical Society Special Reports, 1972.
- (35) Price, W. C. *Annu. Rev. Phys. Chem.* **1960**, *11*, 137.
- (36) (a) Cannon, R. D. *Adv. Inorg. Chem. Radiochem.* **1978**, *21*, 179. (b) Cannon, R. D. *Chem. Phys. Lett.* **1977**, *49*, 299. (c) German, E. D. *Chem. Phys. Lett.* **1979**, *64*, 295.
- (37) Kharats, Yu. I. *Sov. Electrochem. (Engl. Transl.)* **1973**, *9*, 845.
- (38) Vogt, L. H.; Katz, J. L.; Wiberly, S. E. *Inorg. Chem.* **1965**, *4*, 1157. Zalkin, A.; Templeton, D. H.; Adamson, A. *ibid.* **1966**, *5*, 1427.
- (39) Pauling, L. "The Nature of the Chemical Bond"; Cornell University Press: Ithaca, N.Y., 1960.
- (40) Stynes, H. C.; Ibers, J. A. *Inorg. Chem.* **1971**, *10*, 2304.
- (41) (a) Zalkin, A.; Templeton, D. H.; Ueki, T. *Inorg. Chem.* **1973**, *12*, 1641. (b) Baker, J.; Engelhardt, L. M.; Figgis, B. N.; White, A. H. *J. Chem. Soc., Dalton Trans.* **1975**, 530. (c) Saji, T.; Aoyagui, S. *Bull. Chem. Soc. Jpn.* **1973**, *46*, 2101.
- (42) Creutz, C. *Inorg. Chem.* **1978**, *17*, 3723.
- (43) Glick, M. D.; Schmonses, W. G.; Endicott, J. F. *J. Am. Chem. Soc.* **1974**, *96*, 5661.
- (44) Brown, G. M.; Sutin, N. *J. Am. Chem. Soc.* **1979**, *101*, 883.
- (45) Kirkwood, J. G.; Westheimer, F. H. *J. Chem. Phys.* **1938**, *6*, 506.
- (46) Carapellucci, P. A.; Mauzerall, D. *Ann. N.Y. Acad. Sci.* **1975**, *244*, 214.
- (47) Pilling, M. J.; Rice, S. A. *J. Chem. Soc., Faraday Trans. 1* **1975**, *71*, 568. Butler, P. R.; Pilling, M. J.; Rice, S. A.; Stone, T. J. *Can. J. Chem.* **1977**, *55*, 2124.
- (48) Miller, J. R. *J. Phys. Chem.* **1975**, *79*, 1070.
- (49) Fuoss, R. M. *J. Am. Chem. Soc.* **1958**, *80*, 5059. Eigen, M. *Z. Phys. Chem. (Frankfurt am Main)* **1954**, *1*, 176.